

Infrared Spectra of V_nBz_{n+1} Sandwich Clusters: A Theoretical Study of Size Evolution

Jinlan Wang and Julius Jellinek*

Chemistry Division, Argonne National Laboratory, Argonne, Illinois 60439

Received: September 28, 2005

Results of density functional theory computations of infrared (IR) spectra of linear sandwich V_nBz_{n+1} , $n = 1-6$, complexes are presented. It is shown that the systematic changes in the spectra as a function of the complex size can be categorized and understood in terms of responses of the “parent” modes of the Bz molecule and the VBz complex. The analysis presented should be applicable to a broad class of linear sandwich systems.

Introduction

Vanadium–benzene complexes, as representatives of linear sandwich organometallic systems, remain in the focus of an active research effort (see, e.g., refs 1–7 and citations therein). Recent experiments⁵ measured the magnetic moments of V_nBz_{n+1} ($Bz = C_6H_6$) in the size range $n \leq 4$, and a computational study⁶ reexamined the structural, electronic, and magnetic properties of these systems and extended them to $n \leq 6$. The theoretical treatment⁶ has also shown that the measured size-specific values of the magnetic moments⁵ can be understood as averages over different low-energy spin states associated with V_nBz_{n+1} of a given size. An additional, intriguing finding of the theoretical study is that the energetically most stable isomers of V_nBz_{n+1} change at $n = 4$ their achiral D_{6h} structure to the chiral D_2 structure.

What are the implications of this size-induced structural change? Can the theoretical prediction be verified experimentally? Answers to these questions can be given by infrared (IR) spectroscopy.⁸ Clearly, the IR spectrum of the complex evolves with its size. Can we predict through computations the size-induced spectral changes and, even more importantly, understand the reasons and mechanisms underlying them?

IR spectra have been measured and computed for neutral^{7–10} and cationic^{3,4,11,12} VBz and VBz_2 . The goal of this letter is to present density functional theory results on the IR spectra of V_nBz_{n+1} , $n = 1-6$, and to analyze the evolution of these spectra as a function of the complex size. The details and justification of the computational methodology used can be found in ref 6.

Results and Discussion

Here, we present results on IR spectra computed for the most stable isomers of the complex.⁶ The IR active fundamental components of the spectra are shown in the form of stick graphs in Figure 1 (the complete lists of the fundamental modes and their characteristics are given in Supporting Information, Table S1). The figure also displays the available experimental spectral data (“Exp”) for the Bz molecule and the VBz and VBz_2 complexes. These allow one to gauge the accuracy of our

computed results. As is transparent from the figure, these results are in good accord with the measured data (cf. Supporting Information, Table S2). The figure clearly displays size-specific features in the computed spectra and indicates a qualitative change in the pattern at $n = 4$. The high-frequency ν_{20} (in-plane C–H stretching) mode of Bz gets surrounded by very close neighboring modes as n changes from 0 to 6, but its (their) position remains largely unaffected. The low-frequency ν_{23} stretching mode of V–Bz also acquires and shows an overall red shift. Additional IR active modes emerge at $n = 4$ (e.g., ν_6 , ν_8 , and ν_9).

Can these and other size-induced changes in the spectra be understood in terms of the “parent” (or “primitive”) fundamental modes of the constituent Bz and VBz units? The answer to this question is “yes”, and we illustrate this in Table 1 through five representative primitives. Four of them – ν_{11} (out-of-plane CH bending), ν_1 (in-plane ring breathing), ν_{18} (in-plane CH bending), and ν_8 (in-plane ring stretching) – are those of Bz. The fifth is the above-mentioned ν_{23} mode of VBz. A careful analysis of the eigenmodes, which includes visualization, shows that the size-induced changes in the spectra can be categorized into the five types discussed below.

Mode Branching. Some of the new modes of the complex represent a given primitive of a subunit (Bz or VBz) executed in different parts of the complex in an in-phase or anti-phase fashion. This “branching” of the primitives into in-phase and anti-phase daughters is clearly displayed by each of the five parent modes in Table 1.

Mode Combination. New modes also arise as a consequence of different subunits (Bz and VBz), or the same subunit (Bz or VBz) but in different positions, executing different primitive vibrations. The latter, originally of different symmetry, may combine if and when at a certain size of the complex they become of the same symmetry. For this to happen, the complex has to undergo a size-driven structural change. As seen in the table, the primitive $\nu_{23}(A_1)$ mode of VBz becomes a B_1 mode in D_2 -symmetric V_nBz_{n+1} , $n = 4-6$, and it combines with the originally IR inactive primitive $\nu_{16}(E_{2u})$ (out-of-plane C–C–C bending) mode of Bz when in D_2 -symmetric V_nBz_{n+1} complexes ν_{16} splits into B_1 (IR active) and A (IR inactive) components.

* Corresponding author. Phone: 630-252-3463. E-mail: jellinek@anl.gov.

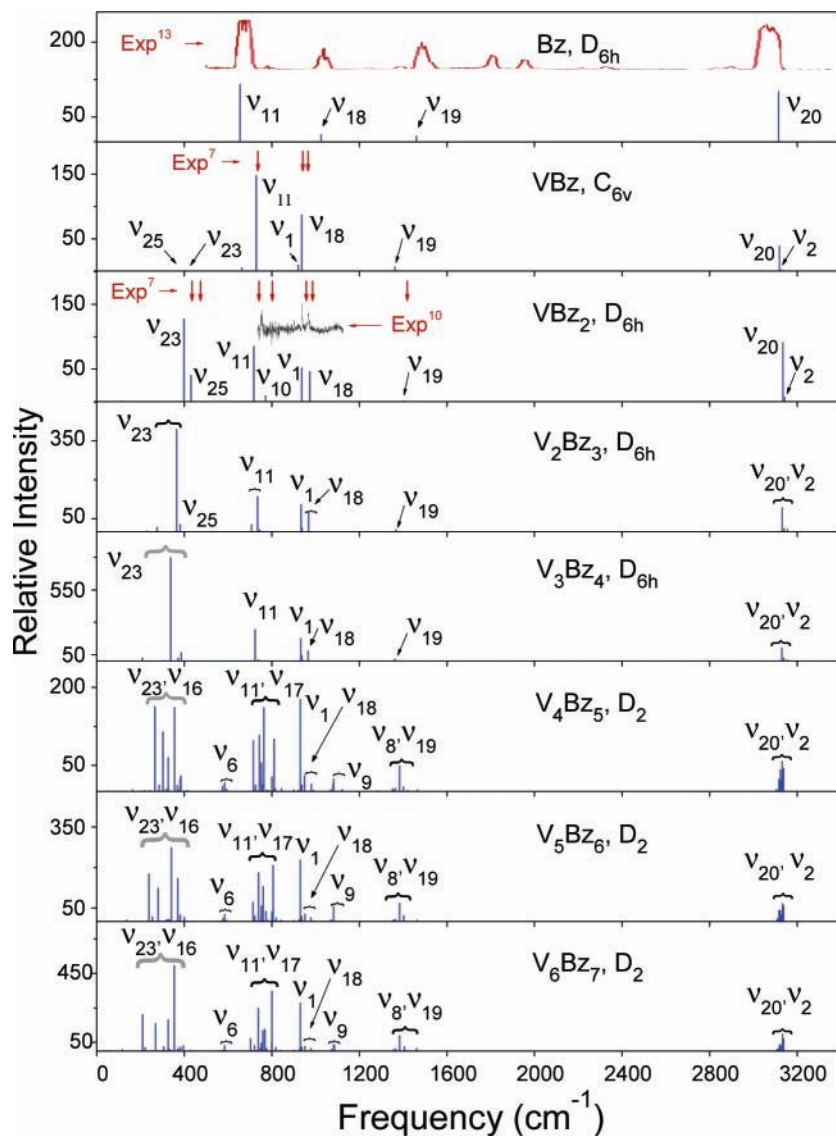


Figure 1. Fundamentals of the computed infrared spectra of the most stable structures of V_nBz_{n+1} (the low-intensity modes may not be seen).

A similar explanation applies to the combination of $\nu_{11}(A_{2u})$ and $\nu_{17}(E_{2u})$ (out-of-plane C–H bending) primitives of Bz in V_nBz_{n+1} , $n = 4-6$.

Mode Splitting. At $n = 4$, the symmetry of the complex is reduced and the degenerate modes split. This is illustrated in the table by the doubly degenerate $\nu_{18}(E_{1u})$ and $\nu_8(E_{2g})$ primitives of Bz. In D_2 -symmetric V_nBz_{n+1} , $n = 4-6$, ν_{18} splits into B_2 and B_3 modes and ν_8 gives rise to B_1 and (an IR inactive) A modes.

IR Inactive-to-Active Switching. ν_{18} and ν_8 also serve as examples of modes that switch from IR inactive to IR active (or vice versa). For $n = 1-3$, the originally IR active $\nu_{18}(E_{1u})$ primitive of Bz branches into IR active E_{1u} and IR inactive E_{1g} modes, which for $n = 4-6$ split into IR active B_2 and B_3 modes. The primitive $\nu_8(E_{2g})$ and its daughter E_{2g} and E_{2u} branches remain IR inactive up to and including $n = 3$. At $n = 4$, both manifolds split into IR active B_1 and IR inactive A modes. Another example is the ν_1 primitive, which is IR inactive in Bz but becomes IR active in VBz and V_nBz_{n+1} (see Table 1). As indicated by the above examples, the reason underlying IR inactive-to-active (or vice versa) switching is the change in the symmetry of a mode as a consequence of either the mode branching discussed above or a change in the point group symmetry of the complex.

Mode Shifting. The size-dependent mode shifting is, in principle, characteristic of every mode. It is monotonic as long as the structural symmetry of the complex remains unchanged, and it may or may not be monotonic across the size (or sizes) at which the complex changes its symmetry. As one would expect, the low-frequency ends of the multiplets formed by branches (combinations) that can be traced to the same primitive mode (modes) shift to the red as V_nBz_{n+1} grows in size. One can notice, though, that the size-induced shift in higher frequency modes shows a tendency to saturate. This can be explained by the finite range of interaction between the constituent VBz units⁶ and only small structural perturbations introduced by high-frequency, small-amplitude modes. The finiteness of the interaction range lends support to the conjecture that the size-induced shift in the low-frequency, large-amplitude modes will also saturate as the length of the V_nBz_{n+1} sandwich continues to increase.

The above discussion identifies the different types of size-specific changes in the spectra based on the responses of the parent modes of the constituent Bz and VBz units. Three of these types – mode combination, mode splitting, and IR inactive-to-active switching – directly relate to the symmetry change in the structure of the complex at $n = 4$.

TABLE 1: Selected Fundamental Modes (in cm^{-1}) of the Most Stable Structures of Bz, VBz, and $V_n\text{Bz}_{n+1}$, $n = 1-6$ (The Symbols Denote the Point Group Symmetry, the Mode Symmetry, and When Needed for Clarity the Reference to Parent Mode(s), and “ia” Stands for “Infrared Inactive”)

mode	Bz(D_{6h})	VBz(C_{6v})	VBz ₂ (D_{6h})	V ₂ Bz ₃ (D_{6h})	V ₃ Bz ₄ (D_{6h})	V ₄ Bz ₅ (D_2)	V ₅ Bz ₆ (D_2)	V ₆ Bz ₇ (D_2)
V-Bz stretching ν_{23}		409(A ₁)	398(A _{2u})	275, 365(A _{2u})	208, 338, 386(A _{2u})	164, 285(ν_{23}), 303, 326, 356($\nu_{23}\oplus\nu_{16}$)(B ₁)	136, 255(ν_{23}), 280, 316, 363, 370($\nu_{23}\oplus\nu_{16}$)(B ₁)	116, 221, 290(ν_{23}), 270, 305, 354, 369($\nu_{23}\oplus\nu_{16}$)(B ₁)
out-of-plane C-H bending ν_{11}	655(A _{2u})	728(A ₁)	716(A _{2u})	708, 734(A _{2u})	703, 732(A _{2u})	715, 725, 742, 752, 763($\nu_{11}\oplus\nu_{17}$)(B ₁)	713, 722, 740, 752, 760, 773($\nu_{11}\oplus\nu_{17}$)(B ₁)	703, 721, 738, 752, 758, 768, 776($\nu_{11}\oplus\nu_{17}$)(B ₁)
in-plane ring breathing ν_1	978(A _{1g} ,ia)	920(A ₁)	937(A _{2u})	933(A _{2u})	906, 931(A _{2u})	900, 931(B ₁)	896, 900, 931(B ₁)	897, 901, 931(B ₁)
in-plane C-H bending ν_{18}	1025(E _{1u})	937(E ₁)	972(E _{1g} ,ia), 974(E _{1u})	938(E _{1u}), 967(E _{1u}), 967(E _{1g} ,ia)	931(E _{1g} ,ia), 936(E _{1u}), 964(E _{1u}), 964(E _{1g} ,ia)	921(B ₂), 929(B ₃), 931(B ₂), 932(B ₃), 935(B ₂), 937(B ₃), 950(B ₂), 950(B ₃), 979(B ₃), 979(B ₂)	919(B ₂), 925(B ₃), 928(B ₃), 929(B ₂), 931(B ₃), 932(B ₂), 934(B ₃), 936(B ₂), 950(B ₃), 950(B ₂), 978(B ₂), 978(B ₃)	917(B ₃), 922(B ₂), 926(B ₃), 928(B ₂), 929(B ₃), 931(B ₂), 932(B ₃), 933(B ₂), 934(B ₃), 936(B ₂), 951(B ₃), 951(B ₂), 978(B ₂), 978(B ₃)
in-plane ring stretching ν_8	1581(E _{2g} ,ia)	1401(E _{2g} ,ia)	1422, 1480(E _{2g} ,ia)	1383(E _{2g} ,ia), 1418(E _{2u} ,ia), 1453(E _{2g} ,ia)	1372(E _{2g} ,ia), 1375(E _{2u} ,ia), 1418(E _{2u} ,ia), 1439(E _{2g} ,ia)	1359, 1363, 1382, 1400, 1464(B ₁)	1357, 1360, 1365, 1382, 1403, 1463(B ₁)	1356, 1360, 1363, 1366, 1383, 1406, 1462(B ₁)

Finally, we remark on the energetically close isomeric forms of $V_n\text{Bz}_{n+1}$.⁶ Since for each size n they are of the same structural symmetry as the most stable structure, and are actually very close to it, their IR spectra are very similar to those shown in Figure 1. Experimental verification of these spectra will serve as a corroboration of the theoretically predicted properties of the complex, including the achiral to chiral change in its structure at $n = 4$.

In summary, we presented computational results on the IR spectra of $V_n\text{Bz}_{n+1}$, $n = 1-6$, and an analysis of their size evolution. We have shown that this evolution can be understood in terms of five types of responses based on the primitive modes of Bz and VBz: (1) mode branching, (2) mode combination, (3) mode splitting, (4) IR inactive-to-active switching, and (5) mode shifting. We expect the description of the size evolution of IR spectra in terms of these responses to be applicable to a broad class of linear sandwich systems.

Acknowledgment. This work was supported by the Office of Basic Energy Sciences, Division of Chemical Sciences, Geosciences, and Biosciences, U.S. Department of Energy, under Contract No. W-31-109-Eng-38.

Supporting Information Available: Complete lists of the computed fundamental modes and their characteristics and comparison of our results with the available experimental and

computed data on IR modes of Bz, VBz, and VBz₂. This material is available free of charge via the Internet at <http://pubs.acs.org>.

References and Notes

- (1) Rabilloud, F.; Rayane, D.; Allouche, A. R.; Antoine, R.; Aubert-Frecon, M.; Broyer, M.; Compagnon, I.; Dugourd, Ph. *J. Phys. Chem. A* **2003**, *107*, 11347.
- (2) Kandalam, A. K.; Rao, B. K.; Jena, P.; Pandey, R. *J. Chem. Phys.* **2004**, *120*, 10414.
- (3) Jaeger, T. D.; Pillai, E. D.; Duncan, M. A. *J. Phys. Chem. A* **2004**, *108*, 6605.
- (4) Jaeger, T. D.; van Heijnsbergen, D.; Klippenstein, S. J.; von Helden, G.; Meijer, G.; Duncan, M. A. *J. Am. Chem. Soc.* **2004**, *126*, 10981.
- (5) Miyajima, K.; Nakajima, A.; Yabushita, S.; Knickelbein, M. B.; Kaya, K. *J. Am. Chem. Soc.* **2004**, *126*, 13202.
- (6) Wang, J.; Acioli, P. H.; Jellinek, J. *J. Am. Chem. Soc.* **2005**, *127*, 2812.
- (7) Lyon, J. T.; Andrews, L. *J. Phys. Chem. A* **2005**, *109*, 431.
- (8) Nakamoto, K. *Infrared and Raman Spectra of Inorganic and Organometallic Compounds*, 5th ed.; Wiley: New York, 1997; Part B.
- (9) Andrews, M. P.; Mattar, S. M.; Ozin, G. A. *J. Phys. Chem.* **1986**, *90*, 744.
- (10) Judai, K.; Sera, K.; Amatsusumi, S.; Yagi, K.; Yasuike, T.; Yabushita, S.; Nakajima, A.; Kaya, K. *Chem. Phys. Lett.* **2001**, *334*, 277.
- (11) Yang, C.-N.; Klippenstein, S. J. *J. Phys. Chem. A* **1999**, *103*, 1094.
- (12) van Heijnsbergen, D.; von Helden, G.; Meijer, G.; Maitre, P.; Duncan, M. A. *J. Am. Chem. Soc.* **2002**, *124*, 1562.
- (13) *NIST Standard Reference Database 69—March 2003 Release: NIST Chemistry WebBook*; <http://webbook.nist.gov>.